Interhead Distances in Myosin Attached to F-Actin Estimated by Fluorescence Energy Transfer Spectroscopy

Shin'ichi Ishiwata,*# Masao Miki,§ Izumi Shin,* Takashi Funatsu,* Kenji Yasuda,¶ and Cristobal G. dos Remedios‖

*Department of Physics, School of Science and Engineering, #Advanced Research Institute for Science and Engineering, and Materials Research Laboratory for Bioscience and Photonics, Waseda University, Shinjuku-ku, Tokyo 169, Japan; §Department of Applied Chemistry and Biotechnology, Fukui University, Fukui-shi 910, Japan; ¶Advanced Research Laboratory, Hitachi Ltd., Saitama, Japan; and ‖Muscle Research Unit, Institute for Biomedical Research, Department of Anatomy and Histology, The University of Sydney, Sydney 2006, Australia

ABSTRACT Fluorescence resonance energy transfer (FRET) spectroscopy has been used to determine distances between probes attached to the most reactive sulfhydryl (SH1) group on individual myosin "heads." We measured intramolecular and intermolecular interhead distances as well as the distance between one head of heavy meromyosin (HMM) mixed with subfragment-1 (S1) heads attached to F-actin under rigor conditions. The SH1 cysteine was specifically labeled with either a donor (5-((((2-iodoacetyl)amino)ethyl)amino)naphthalene-1-sulfonic acid) or an acceptor probe (5-iodoacetamidofluorescein). In free solution, the distance between these probes was too large to allow significant FRET, but in the rigor complex with F-actin, intermolecular interhead distances between S1 molecules, HMM molecules, or S1 and HMM were determined to be 6.0–6.3 nm. The radial coordinate of the labels relative to F-actin was 5.0–6.4 nm. However, the intramolecular interhead distance in HMMs in which the two heads were labeled with D and A probes was estimated to be larger. The binding affinity of the second head of HMM(D/A) to F-actin may be reduced because of heterogeneous modification of the SH1 groups, such that the probability of single-head binding is increased.

INTRODUCTION

The attachment of myosin heads to F-actin is a key step in the molecular process involved in muscle contraction and the development of contractile force. Any investigation that reveals structural relationships between these two proteins would surely provide valuable insights into this molecular process. In recent years our understanding of the structure of actin (Kabsch et al., 1990; McLaughlin et al., 1993; Schutt et al., 1993) has advanced to the point where there is no longer room for reasonable doubt. The three-dimensional structure of subfragment-1 (S1) of myosin (Rayment et al., 1993b) has been resolved by x-ray crystallography such that we now have a clear picture of the separate proteins. This has naturally led to speculation as to the atomic structure of F-actin (Holmes et al., 1990; Lorenz et al., 1993; Tirion et al., 1995) and of the acto-S1 complex (Rayment et al., 1993a; Schröder et al., 1993; see dos Remedios and Moens, 1995a, for a full review).

The atomic structure of these complexes will remain unsolved until high-resolution data become available from F-actin and the acto-S1 complex when, and if, they are crystallized. However, electron microscopy of SH1-biotin-avidin-labeled S1 revealed that the most reactive SH1 cysteine (Cys707) and the ATP-binding sites are both located at a position approximately one-third the length of S1 from the tip of the head (Sutoh et al., 1984, 1986). Using the same technique, the geometrical relationships among the actin-binding site, ATP-binding site, and SH1 on S1 in the actin-tropomyosin-S1 complex were also investigated (Tokunaga et al., 1987; Toyoshima et al., 1985). These results are consistent with the more recent three-dimensional reconstruction of unstained S1-decorated F-actin observed by cryoelectron microscopy and with the known structure of S1 (Rayment et al., 1993a; Schröder et al., 1993).

Fluorescence resonance energy transfer (FRET) spectroscopy has been widely used to study the spatial relationships between specific sites in proteins. In particular, FRET has been employed to study distances between a large number of loci on myosin and actin (cf. dos Remedios et al., 1987; Miki et al., 1992; dos Remedios and Moens, 1995b). Among these, the SH1 residue is by far the most well characterized. It is located in a section of α-helix on the 20-kDa segment lying under the nucleotide-binding site pocket. Chemical modification of SH1 modifies the ATPase activity of S1 (Kielley and Bradley, 1956; Seidel, 1969). Thus we elected to study the acto-S1 (or heavy meromyosin, HMM) rigor complex without nucleotides.

An important innovation of the FRET technique is its capacity to determine the radial coordinate of a pair of loci with respect to the axis of the actin filament. This was first done by Taylor et al. (1981) for a donor and acceptor probe pair located at residue Cys374 on F-actin under conditions ensuring random assembly. Kasprzak et al. (1988) and Moens et al. (1994) studied this locus using different probe pairs. Besides Cys374, the radial coordinates of other loci

Received for publication 15 October 1996 and in final form 15 May 1997.

Address reprint requests to Dr. Shin'ichi Ishiwata, Department of Physics, School of Science and Engineering, Waseda University, 3-4-1 Okubo, Shinjuku-ku, Tokyo 169, Japan. Tel.: 81-3-5286-3437; Fax: 81-3-3200-2567; E-mail: ishiwata@mn.waseda.ac.jp.

Dr. Funatsu's present address is Yanagida Biomotron Project, ERATO, JRDC, 2-4-14 Senba-Higashi, Mino, Osaka 562, Japan.

0006-3495/97/08/895/10 $2.00

on F-actin have been determined, including Cys10, Gln41, Tyr69, and the nucleotide-binding site on F-actin (for a review, see Miki et al., 1992). These observations raised the possibility of determining the radial coordinates of SH1 on S1 in a rigor complex with F-actin, provided that the donor-acceptor probe pair does not exceed the outer limit imposed by the Förster (1965) critical distance (R_0) relationship. The probe pair used in this report effectively limits our measurements to ~7.5 nm.

In the absence of ATP, myosin forms a tight complex with F-actin, which saturates at one head per actin monomer. Assuming the above location of SH1 on the S1, determination of its radial coordinate would require that the donor-acceptor probe pair be able to sense distances longer than those used to determine the radial coordinates of loci on F-actin. Furthermore, the determination of the radial coordinate would only be possible if the next myosin "head" bound to the nearest-neighbor actin monomer under conditions in which a head is bound to all monomers in F-actin. Binding to any other monomer (e.g., one on the opposite strand of the two-start helix) would be too great a distance for the FRET method.

Herein we present evidence which strongly suggests that the two "heads" of myosin do indeed bind to adjacent actin monomers on the long-pitch helix of F-actin. In addition, we present a new insight into the binding mode of two heads, based on interpretation of the experimental data according to a model simulation.

Preliminary results were previously published as abstracts (Ishiwata et al., 1987b, 1988, 1996). The intermolecular distance between S1 molecules attached to F-actin was recently measured by Brown and Hambly (1996) with a similar technique.

MATERIALS AND METHODS

Chemicals

5-((((2-Iodoacetyl)amino)ethyl)amino)naphthalene-1-sulfonic acid (1,5-IAEDANS) and 5-iodoacetamidofluorescein (5-IAF) were purchased from Molecular Probes (Eugene, OR). DE52 was obtained from Whatman BioSystems (Maidstone, Kent, England), trypsin was from Sigma Chemical Co. (St. Louis, MO), and α-chymotrypsin was from Worthington Biochemical Co. (Freehold, NJ). Hydroxylamine hydrochloride was purchased from Wako Pure Chemical Industries (Osaka, Japan), and piperazine-*N*,*N*′-bis(2-ethanesulfonic acid) (PIPES) was from Sigma Chemical Co. or Dojindo Lab. (Kumamoto, Japan). All other chemicals were of analytical grade.

Protein preparations

Myosin and actin were prepared from rabbit back and leg white muscles as previously reported (Kinosita et al., 1984). Myosin was stored in 50% glycerol at −20°C. Glycerol was removed by precipitating myosin in 50 mM KCl and 5 mM PIPES (pH 7.0) (solution A) with low-speed centrifugation at 4°C just before use. In some preparations, myosin was chromatographed on DE52, but the results were indistinguishable from those obtained by using myosin prepared without column chromatography. F-actin was generated from G-actin by the addition of 50 mM KCl, 2 mM $MgCl_2$, and 50 mM PIPES (pH 7.0). Molecular masses used for calculating molar concentrations of proteins were 115 kDa for S1, 350 kDa for HMM, 480 kDa for myosin, and 42 kDa for actin. Protein concentrations were determined by the biuret method, as well as by using the extinction coefficients of $A^{1\%}_{290\ nm} = 6.3\ cm^{-1}$ for G-actin (Lehrer and Kerwar, 1972), $A^{1\%}_{280\ nm} = 7.5\ cm^{-1}$ for S1 (Weeds and Pope, 1977), and 6.0 cm^{-1} for HMM (Margossian and Lowey, 1978).

Labeling of proteins

The following five different samples were prepared as schematically illustrated in Fig. 1 (see Table 1):

1. double-labeled HMM in which 9–15% of heads were labeled with IAEDANS (D) and 60–85% with IAF (A) (HMM(D/A));
2. labeled HMM in which 69–93% of heads were labeled with D (HMM(D)) or A (HMM(A));
3. labeled S1 in which 70–83% was labeled with D (S1(D)) or A (S1(A)).

Labeled HMM and S1 were prepared by chymotryptic digestion of labeled myosin as previously reported (Kinosita et al., 1984). For the preparation of HMM(D/A), 10 mg/ml (~42 μM heads) of myosin was first mixed with 4 or 8 μM IAEDANS (10–20% molar ratios of label/myosin heads) in solution A with 0.1 mM EDTA for 3 h. Free dyes were removed by repeatedly sedimenting myosin under low-salt conditions followed by dissolution at a high-salt concentration (0.6 M KCl, 20 mM PIPES, pH 7.0). IAEDANS-labeled myosin was mixed with a threefold molar excess of IAF in solution A with 0.1 mM EDTA for 16 h. The reaction was terminated by the addition of 1 mM dithiothreitol, and free dyes were removed by repeated sedimentation as described above. The final pellet was dissolved in the above high-salt solution, and undissolved aggregates were removed by ultracentrifugation at 100,000 × g for 1 h; then the supernatant was dialyzed against the same high-salt solution containing 1 mM $MgCl_2$. Probes were dissolved in dimethylformamide (DMF) and slowly added to the myosin solution with continuous stirring. The volume of DMF added did not exceed 1% (v/v) of the total volume. All procedures were carried out at 4°C in the dark. The fraction of heads labeled with D was estimated before the addition of A because the absorption coefficient of D is an order of magnitude smaller than that of A.

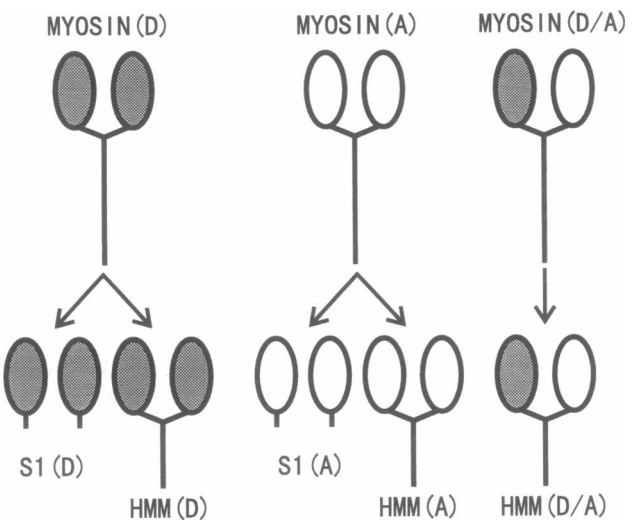

FIGURE 1 Protocol for labeling S1 and HMM with a fluorescence donor (D), IAEDANS, and a fluorescence acceptor (A), IAF. Cys707 (SH1) of myosin was labeled with either D (MYOSIN(D)) or A (MYOSIN(A)), or double-labeled with A after labeling with D (MYOSIN(D/A)). Then five different samples, S1(D), HMM(D), S1(A), HMM(A) and HMM(D/A), were prepared by chymotryptic digestion. Myosin heads labeled with D are represented by filled ovals, those labeled with A by unfilled ovals.

TABLE 1 Characterization of labeled myosin heads

Sample	Fraction of labeled heads*	Relative K^+-EDTA-ATPase rates#	Relative Ca^{2+}-ATPase rates§
S1 (unlabeled)	—	1	1 (1)
S1(D)	81.3	0.19 (81)	2.54 (2.98)
S1(A)	85.0	0.09 (91)	1.40 (2.93)
HMM(D)	79.0	0.30 (70)	2.39
HMM(A)	92.8	0.10 (90)	1.71
HMM(D/A)	15.0/80.0	0.07 (93)	2.35

*Expressed as a percentage of the ratio between molar concentrations of dyes and myosin heads. For details, see Materials and Methods.
#Relative values of ATPase rates measured in 0.45 M KCl, 5 mM ATP, 0.5 mM Tris-HCl (pH 8.0) and 1 mM EDTA at 20°C. Values in parentheses (%) are the fraction of labeled heads estimated by assuming that labeled heads lost their ATPase activity.
§Relative values of ATPase rates measured in 0.6 M KCl, 5 mM ATP, 0.5 mM Tris-HCl (pH 8.0) and 10 mM $CaCl_2$ at 20°C or 30°C (values in parentheses).

Molar labeling ratios of double-labeled HMM heads were, for example, 0.15 for D and 0.80 for A (Table 1). Here we assumed that the labeling occurs at random, such that the fraction of HMM(D/A) in which one head was labeled with D and the other with A was estimated to be 0.24 ($0.15 \times 0.80 \times 2$), the fraction in which both heads were labeled with D was 0.02 (0.15×0.15), that with A was 0.64 (0.80×0.80), and the fraction in which one of the two heads was unlabeled was 0.1. Extinction coefficients of 6,100 M^{-1} cm^{-1} at 338 nm for IAEDANS (Hudson and Weber, 1973) and 75,000 M^{-1} cm^{-1} at 490 nm for IAF (Takashi, 1979) were used to determine the labeling ratios.

Spectroscopic measurements

Absorption was measured with an ultraviolet/visible spectrophotometer, either a Philips PU 8800 or a Shimadzu UV 2100. Fluorescence intensity was measured with a photon counting SLM 8000 spectrofluorometer (Urbana, IL) operated in the ratio mode or with a Hitachi 240-60 spectrofluorometer (Hitachi Ltd., Tokyo). Light scattering intensity was measured at 550 nm at a 90° angle, using the latter spectrofluorometer. The temperature was maintained at 20°C.

Fluorescence resonance energy transfer

The efficiency (E) of FRET between probes was determined by measuring the fluorescence intensities (F) of the donor, in both the presence (F_{DA}) and the absence (F_D) of the acceptor, as given by

$$E = 1 - F_{DA}/F_D$$

E is related to the distance (R) between a donor and an acceptor and the Förster (1965) critical distance (R_0), at which E is equal to 0.5, as follows:

$$E = R_0^6/(R_0^6 + R^6)$$

R_0 (in nm) can be obtained by

$$R_0^6 = (8.79 \times 10^{-11})n^{-4}\kappa^2 Q_0 J$$

where n is the refractive index of the medium (taken to be 1.4), κ^2 is the orientation factor, Q_0 is the quantum yield of the donor in the absence of the acceptor, and J is the spectral overlap integral (in M^{-1} cm^{-1} nm^4) between donor emission and acceptor absorption. The quantum yield of IAEDANS bound to S1 was taken to be 0.44, as previously reported (Miki, 1987). κ^2 was assumed to be 2/3 for calculation of the distance R_0. In the present case, R_0 was calculated to be 4.81 nm. Thus the effective upper limit of R was ~7.5 nm.

SDS PAGE

To examine the specificity of labeling, sodium dodecyl sulfate (SDS)-polyacrylamide gel electrophoresis (PAGE) was performed according to the method of Laemmli (1970), with slight modifications (Kinosita et al., 1984). Acrylamide concentrations were 15% (w/v) for the separating gel and 5% (w/v) for the stacking gel. Coomassie Brilliant Blue R-stained SDS-PAGE gels were photographed with a Polaroid camera (600SE), using a positive/negative instant film (Polaroid 665). Fluorescent bands were photographed on a trans-illuminator (model TL-33 with 365 nm; Ultra-violet Products). SDS-PAGE in urea was performed, using 16% and 5% (w/v) acrylamide for the separating and stacking gels, respectively (Sutoh, 1981).

Other techniques

ATPase activities of unlabeled and labeled S1 and HMM were measured using a pH stat consisting of a Radiometer TTT2 titrator with a PHA943 titrigraph module, an ABU12 autoburette, and an SBR3 titrigraph assembly (Miki, 1987). The activities of labeled myosin fragments are reported relative to that of unlabeled S1 (or in the case of HMM, twice that of unlabeled S1). The binding of HMM to F-actin was determined from the protein concentration in the supernatant obtained after ultracentrifugation at 160,000 × g for 40 min at 20°C (TL-100, Beckman).

Data analysis and estimation of interhead distance

The FRET data were analyzed by model simulation. First we assumed that FRET occurs between adjacent (nearest-neighbor) S1 fragments and the heads of HMM bound to the long-helical strand of F-actin, because the FRET efficiency (E) would be negligibly small for second-nearest neighbors. Our experimental design did not require taking into account cooperative binding of S1 (or HMM) molecules to F-actin, at least at molar ratios of F-actin/S1 (or heads of HMM) below 1, because virtually all of the F-actin sites were occupied by bound S1 (and/or HMM). The actual degree of occupancy depends on the binding constant under rigor conditions. Under our experimental conditions, it could be assumed that the fraction of A-labeled heads adjacent to a D-labeled head on an F-actin is equal to the fraction of attached A-labeled heads. Thus we were able to analyze the data according to the binding equilibrium equations assuming random binding between S1 (and/or HMM) molecules and F-actin. The following exemplifies our approach.

1. Consider S1 binding to F-actin (FA):

$$\text{FA} + \text{S1} \leftrightarrow \text{FA-S1}: \quad K[\text{FA}][\text{S1}] = [\text{FA-S1}]$$

where we assumed that the binding constant K does not depend on whether S1 is labeled. The total concentrations of actin ($[FA_0]$) and S1 ($[S1_0]$) are

$$[\text{FA}_0] = [\text{FA}] + [\text{FA-S1}]$$

$$[\text{S1}_0] = [\text{S1}] + [\text{FA-S1}]$$

$$[\text{FA-S1}] = [\text{FA-S1(D)}] + [\text{FA-S1(A)}] + [\text{FA-S1(U)}]$$

$$[\text{S1}] = [\text{S1(D)}] + [\text{S1(A)}] + [\text{S1(U)}]$$

where S1(U) indicates unlabeled S1. By solving these equations, we determined the concentrations of each species.

Here the fluorescence intensity (F) of D is represented by the following equation:

$$F([\text{FA}_0], f) = [\text{S1(D)}] + a[\text{FA-S1(D)}]G(f)$$

where f is the fraction of actin-binding sites with attached S1(A), i.e., $f = [\text{FA-S1(A)}]/[\text{FA}_0]$; a is the ratio of fluorescence intensities of D in attached

and detached states in the absence of A, i.e., $a = F(\text{FA-S1(D)})/F(\text{S1(D)})$, which was determined to be 1.1. $G(f)$ is a factor contributing to a decrease in fluorescence intensity due to the FRET between each donor and adjacent acceptor(s) in the rigor complex with F-actin:

$$G(f) = (1-f)^2 + 2f(1-f)/\{1 + (R_0/R)^6\} + f^2/\{1 + 2(R_0/R)^6\}$$

where R_0 is the Förster critical distance (i.e., 4.81 nm) for the combination of IAEDANS and IAF. In practice, F was examined after normalization with the F of S1(D) measured in the absence of S1(A) at the same $[FA_0]$.

2. Next we briefly present the case of HMM:

$$FA + HMM \leftrightarrow FA\text{-}HMM: K'[FA][HMM] = [FA\text{-}HMM]$$

where we assumed that the binding constant K' does not depend on whether both heads of HMM are labeled with D (HMM(D)) or A (HMM(A)) or are unlabeled (HMM(U)), or only one head is labeled with either D or A, and the other head is unlabeled (HMM(D/U) or HMM(A/U), respectively). The total concentrations of actin ($[FA_0]$) and HMM ($[HMM_0]$) are

$$[FA_0] = [FA] + 2[FA\text{-}HMM]$$

$$[HMM_0] = [HMM] + [FA\text{-}HMM]$$

$$[FA\text{-}HMM] = [FA\text{-}HMM(D)] + [FA\text{-}HMM(A)] + [FA\text{-}HMM(U)] + [FA\text{-}HMM(D/U)] + [FA\text{-}HMM(A/U)]$$

$$[HMM] = [HMM(D)] + [HMM(A)] + [HMM(U)] + [HMM(D/U)] + [HMM(A/U)].$$

Other formulations are essentially the same as that for case 1, that is,

$$F([FA_0], f) = 2[HMM(D)] + [HMM(D/U)] + a\{2[FA\text{-}HMM(D)] + [FA\text{-}HMM(D/U)]\}G(f)$$

and

$$G(f) = (1-f) + f/\{1 + (R_0/R)^6\}$$

where $f = \{2[\text{FA-HMM(A)}] + [\text{FA-HMM(A/U)}]\}/[FA_0]$.

For data analysis, the above F was normalized by dividing it by the F of HMM(D), measured in the absence of HMM(A) at the same $[FA_0]$.

The interhead distance obtained in this study depended on the values of the chosen binding constants. The larger (or smaller) the value of the binding constants we assumed, the longer (or shorter) were the interhead distances. However, the maximum deviation of 0.1 nm was estimated for the interhead distances for binding constants ×2 or ×0.5 the assumed values. Taking into account the published binding constants (Marston and Weber, 1975; Highsmith, 1977, 1978; Margossian and Lowey, 1978; Miyanishi and Borejdo, 1989) and comparing the light scattering and simulated curves shown in Figs. 3–7, we determined that the combination of $K = 10^7/M$ and $K' = 5 \times 10^7/M$ best fits the data.

On the other hand, we assumed that the light scattering intensity increases in proportion to the attached S1 and HMM heads in which, for the sake of simplicity, their different contributions to the light scattering intensity were not taken into account.

By assuming a helical symmetry for SH1 groups around an actin filament (Fig. 2), their average radial coordinate, q, about the actin filament can be estimated (Taylor et al., 1981) by

$$R^2 = (2q \sin(\phi/2))^2 + P^2$$

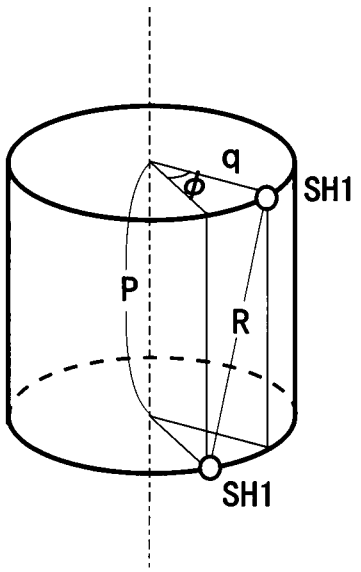

FIGURE 2 A schematic illustration of the geometry of the location of SH1 of myosin heads when attached to F-actin. The vertical broken line represents the central axis of F-actin; R, the distance between adjacent SH1 groups of myosin heads; P, the pitch of an actin molecule in F-actin, 5.5 nm; ϕ, 28°. We assumed that the arrangement of myosin heads around F-actin has helical symmetry and that SH1 is located on a cylinder with a radius (radial coordinate) of q.

where R is the distance between adjacent SH1 sites, q is the radial coordinate of the probe with respect to the actin filament axis, the angle ϕ (=28°) is the rotation of one monomer with respect to the next monomer along the same long-pitch strand, and P (=5.5 nm) is the pitch of an actin monomer along a long-pitch helical strand of F-actin. These parameters are defined in Fig. 2.

RESULTS

Characterization of labeled myosin

SDS PAGE showed that the labels were selectively incorporated into SH1 of myosin heavy chains (data not shown). Labeled S1 was digested with trypsin and further treated with hydroxylamine for 5.5 h at 45°C. Our observations were in accordance with those of Sutoh (1981), who previously showed the 20-kDa fragment of the S1 heavy chain, which contains the two "essential" thiol groups SH1 and SH2, to be fragmented by hydroxylamine treatment into a 13-kDa peptide containing SH1 and a 7-kDa peptide containing SH2. Only the 20-kDa and 13-kDa fragments were fluorescent, indicating that both labels are selectively attached to SH1.

The K^+-EDTA-ATPase and Ca^{2+}-ATPase activities of SH1-labeled S1 and HMM were compared with those of unlabeled S1 (Table 1). The decrease in K^+-EDTA ATPase activity of labeled S1 and HMM was consistent in relationship to the fraction of labeled heads estimated from spectroscopic data. On the other hand, the Ca^{2+}-ATPase activities of labeled S1 and HMM were greater than that of unlabeled S1. These results also indicated a specific labeling

of SH1 under our present experimental conditions (Sekine and Kielley, 1964; Seidel, 1969). It should be noted that the extent of the increase in Ca^{2+}-ATPase activity induced by SH1 labeling strongly depends on the species of labeling dyes and on the temperature (especially in the case of IAF) at which the ATPase measurements are carried out.

The shape of the absorption and emission spectra of HMM, double-labeled with IAEDANS (D) and IAF (A), was the superposition of the spectra of HMM labeled with either D or A. Throughout these experiments, the fluorescence intensity of IAEDANS was measured at 470 nm (the noise level was ~1% of the signal level), with excitation at 338 nm, the wavelength at which there was no contribution from the fluorescence of IAF (spectra, not shown).

FRET between intermolecular heads of S1(D) and S1(A) attached to F-actin

The change in fluorescence intensity of IAEDANS-labeled S1 (S1(D)) in the mixture with IAF-labeled S1 (S1(A)) after the addition of F-actin was measured under rigor conditions. As shown in Fig. 3, the normalized fluorescence intensity ($F_{DA}/F_D = 1 - E$) decreased as the molar ratios of actin to S1 increased up to 1, and then increased again to nearly the initial value. With this change, the light scattering intensity increased and saturated at a molar ratio of ~1. The recovery of fluorescence intensity at molar ratios of >1 can be attributed to a decrease in the fraction of neighboring S1(A) on the F-actin filaments. This is shown schematically in the inset in Fig. 3. Ultracentrifugation of the F-actin/S1 complex at a molar ratio of 1:1 showed that ~95% of S1 cosedimented with F-actin, demonstrating that 95% of the heads were attached to F-actin, leaving ~5% of S1 in the supernatant.

The data were analyzed according to the random attachment model described in Materials and Methods. Three curves superimposed on the data indicated that the average interhead distance (= distance between nearest-neighbor SH1s) is 6.2 nm (corresponding radial coordinate, q = 5.9 nm), although the data deviated from the simulated curve, especially at higher molar ratios of F-actin and S1. Here and below, we present a set of data obtained by using a preparation with a certain D/A labeling ratio, except in the case of HMM(D/A); although we did not obtain duplicate data for every point, some duplicate data suggest that the estimation error for donor-acceptor distances is within the range of the three calculated curves shown in the figures.

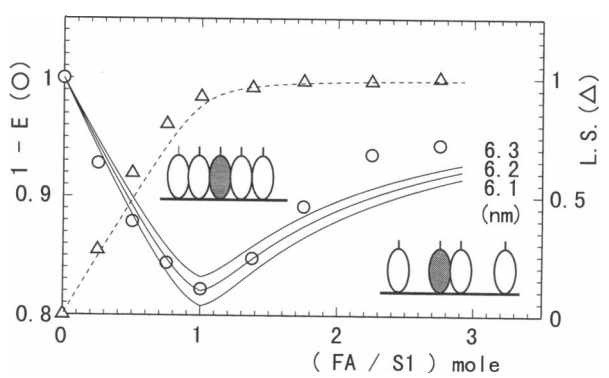

FIGURE 3 Change in FRET efficiency (E) between S1(D) and S1(A) induced by the addition of F-actin (○) under rigor conditions. The binding of S1 and F-actin was monitored by light scattering intensity (LS) at 550 nm (△). S1(D), 73% labeled with IAEDANS; S1(A), 70% labeled with IAF. A small volume of 7 mg/ml (167 μM) of F-actin solution (0.1 M KCl, 1 mM $MgCl_2$, 20 mM Tris-HCl, pH 8.0, 0.1 mM ATP) was added stepwise (final concentration 17 μM) to the solution containing 0.035 mg/ml (0.3 μM) S1(D) and 0.7 mg/ml (6 μM) of S1(A) dissolved in 0.1 M KCl, 1 mM $MgCl_2$, 20 mM Tris-HCl (pH 8.0) at 20°C. The fluorescence intensity was measured after hydrolysis of contaminant ATP. Dilution effects were taken into consideration. The inset illustrates schematically the binding of S1 to F-actin (see Fig. 1). The three curves obtained by model simulation are superimposed on the data. The distance between adjacent S1(D) and S1(A) used for obtaining each curve is shown on the right-hand side.

FRET between intermolecular heads of S1(D) and HMM(A) attached to F-actin

The FRET was determined for a mixture of S1(D) and HMM(A) in the presence of various amounts of F-actin under rigor conditions. As shown in Fig. 4, the normalized fluorescence intensity decreased with increasing molar ratios of F-actin to heads (S1(D) + heads of HMM(A)) up to 1 and then increased again to nearly the initial value. Note that the decrease in fluorescence intensity as the molar ratios approached 1 was convex upward, which contrasts with the S1(D)/S1(A) case in which the decrease was slightly concave (Fig. 3; a characteristic curve was also distinct in other preparations). The simulation curve can reproduce these characteristics. In addition, the average interhead distance was estimated to be 6.3 nm, which is nearly equal to that observed for the S1(D)/S1(A) case. On the other hand, the light scattering intensity increased linearly and saturated when the molar ratio of actin and heads

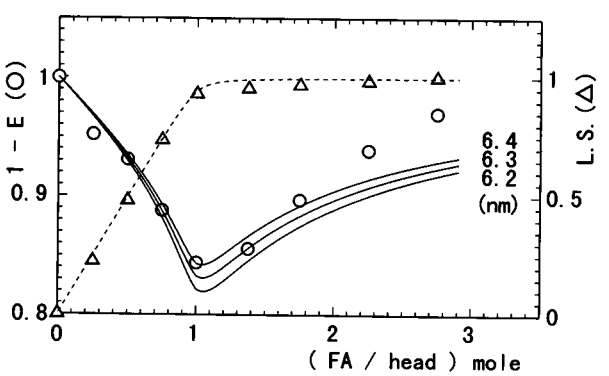

FIGURE 4 Change in FRET efficiency (E) between S1(D) and HMM(A) induced by the addition of F-actin (○) under rigor conditions. The binding of S1 and HMM to F-actin was monitored by light scattering intensity at 550 nm (△). Other conditions and experimental procedures were the same as in Fig. 3, except that 1.05 mg/ml (3 μM = 6 μM heads) of 69% labeled HMM(A) was used instead of S1(A). The abscissa shows the numerical ratio of added actin against S1(D) plus heads of HMM(A).

was 1, suggesting a 1:1 stoichiometry for myosin heads bound to F-actin, similar to the S1(D)/S1(A) case (Fig. 3). The major difference from this latter case is the steep curve around molar ratios of 1, indicating a large HMM binding constant.

FRET between intermolecular heads of HMM(D) and S1(A) attached to F-actin

Similar experiments were performed using mixtures of HMM(D) and S1(A). As shown in Fig. 5, the normalized fluorescence intensity decreased as the molar ratios of actin monomers to heads (S1(A) + heads of HMM(D)) increased up to 1, and then increased again to nearly the initial value. There is a clear concave, although smaller, decrease in fluorescence intensity (up to 0.9). Despite this, the calculated average interhead distance was similar, i.e., ~6.1 nm. In addition, the light scattering intensity data confirmed that binding stoichiometry occurs at a molar ratio of actin monomers to heads of ~1.

FRET between intermolecular heads of HMM(D) and HMM(A) attached to F-actin

Experiments were done for the fourth combination of heads, using a mixture of HMM(D) and HMM(A). As shown in Fig. 6, the normalized fluorescence intensity decreased with an increase in the molar ratios of actin monomers to total heads, and then increased above molar ratios of 1. The average interhead distance obtained by the model simulation produced a value similar to those of the above combinations, i.e., ~6.0 nm. Changes in light scattering intensity were similar to those of the other cases, although the data points were slightly more scattered and a gradual decrease was seen above molar ratios of 1.

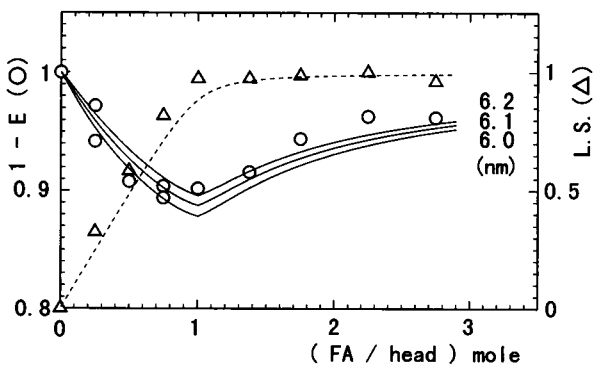

FIGURE 5 Change in FRET efficiency (E) between HMM(D) and S1(A) induced by the addition of F-actin (○) under rigor conditions. The binding of HMM and S1 to F-actin was monitored by light scattering intensity at 550 nm (△). Other conditions and experimental procedures were the same as in Fig. 3, except that 0.056 mg/ml (0.16 μM = 0.32 μM heads) of 78% labeled HMM(D) was used instead of S1(D). The abscissa shows the numerical ratio of added actin against S1(A) plus heads of HMM(D).

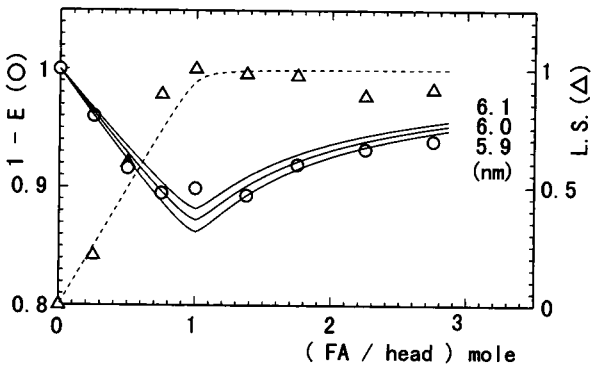

FIGURE 6 Change in FRET efficiency (E) between HMM(D) and HMM(A) induced by the addition of F-actin (○) under rigor conditions. The binding of HMM to F-actin was monitored by light scattering intensity at 550 nm (△). Other conditions and experimental procedures were the same as in Fig. 3, except that 0.056 mg/ml (0.16 μM = 0.32 μM heads) of 78% HMM(D) and 1.05 mg/ml (3 μM = 6 μM heads) of 69% labeled HMM(A) were used instead of S1(D) and S1(A), respectively. The abscissa shows the numerical ratio of added actin against heads of HMM(D) and HMM(A).

FRET between intramolecular heads in HMM attached to F-actin

Using the techniques described above, we designed experiments to determine the intramolecular interhead distance (R_{intra}) of HMM molecules attached to F-actin, complementing the intermolecular interhead distance (R_{inter}) obtained above. Fig. 7 summarizes the results of the fluores-

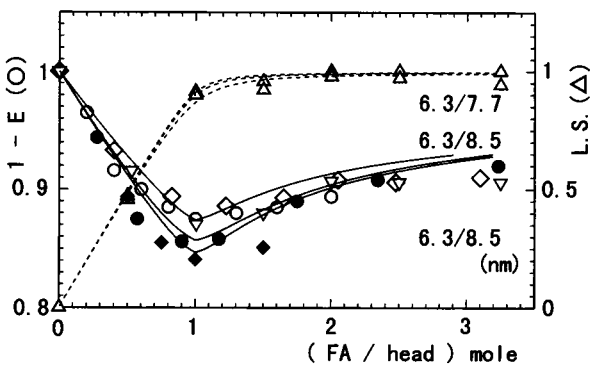

FIGURE 7 Change in FRET efficiency (E) within and between HMM(D/A) molecules induced by the addition of F-actin (●, ◆, ○, ◇, ▽) under rigor conditions. The binding of HMM to F-actin was monitored by light scattering intensity at 550 nm (△). Other conditions and experimental procedures were the same as in Fig. 6, except that double-labeled HMM(D/A) was used instead of HMM(D) and HMM(A). Three different HMM(D/A) preparations were examined: ●, ◆, 0.40 mg/ml (1.15 μM = 2.3 μM heads) HMM(D/A) containing 9% D and 85% A, F-actin was added stepwise up to 7.36 μM; ○, ◇, 0.175 mg/ml (0.5 μM = 1.0 μM heads) HMM(D/A) containing 15% D and 80% A, F-actin was added stepwise up to 3.2 μM; ▽, 0.30 mg/ml (0.86 μM = 1.7 μM heads) HMM(D/A) containing 15% D and 60% A, F-actin was added stepwise up to 5.2 μM. A model simulation was done for each preparation. The distance corresponding to each curve is shown on the right-hand side, with the intermolecular interhead distance (R_{inter}) being shown on the left-hand side and the intramolecular interhead distance (R_{intra}) on the right.

cence intensity and light scattering experiments with three different D/A ratios. A range of different protein concentrations was examined to test the suitability of the model simulations. We anticipated that the results (Fig. 7) would mirror those described above. However, the data unexpectedly resulted in an average interhead distance of 7.0 nm, rather than the 6.0–6.3 nm obtained above. The best fit of the simulation curves to the data is shown here (Fig. 7). We have made the reasonable assumption that the distance between heads on different molecules (R_{inter}) remained at 6.3 nm. Note that a similar interhead distance was obtained, irrespective of the fraction of donor-labeled and acceptor-labeled heads produced in the HMM population.

FRET between intramolecular heads in free HMM

These experiments were designed to distinguish between D/A labeled heads that were not constrained by binding to F-actin. Thus we attempted to determine whether FRET occurs between heads within free HMM molecules in the absence of F-actin. For this purpose, we compared the time course of fluorescence intensity changes in double-labeled HMM(D/A) molecules with that of HMM(D) after the addition of trypsin (Chantler and Tao, 1986). Had FRET occurred between the unattached heads of HMM, the ratio of the fluorescence intensities for HMM(D/A) and HMM(D) would presumably have increased, because the FRET efficiency would have decreased because of the separation of heads by limited tryptic digestion. The results (data not shown) revealed a decrease in fluorescence intensity of HMM(D/A) similar to that observed with HMM(D). Thus no appreciable change in the ratio of fluorescence intensities was detected.

DISCUSSION

Characteristics of SH1-labeled myosin

Since Sekine and Kielley (1964) first demonstrated that specific modification of SH1 on myosin heads with *N*-ethylmaleimide activates the Ca^{2+}-promoted ATPase activity of myosin while inhibiting the K^+-EDTA ATPase activity, many researchers have used this property to identify the specific labeling of this locus with fluorescent dyes (dos Remedios et al., 1987). Therein we have shown that the extent of the activation of the Ca^{2+}-ATPase activity by SH1 modification depends on the labeling dyes used and on the temperature at which the ATPase activity is measured (Table 1). This was also the case for the labeling of SH1 of S1 with IANBD, in which the Ca^{2+}-ATPase activity of IANBD-S1 was less than that of unlabeled S1 at 20°C and was 1.7 times that of unlabeled S1 at 38°C (Miki and Wahl, 1984). Thus these properties of the Ca^{2+}-ATPase activity must be considered for identifying the specific SH labeling.

Estimation of interhead distance by FRET

In the FRET analysis, κ^2 was assumed to be ⅔. The upper and lower bounds of this parameter were calculated according to the method of Dale et al. (1979). The limiting anisotropies of IAEDANS and IAF bound to SH1 were previously determined to be 0.283 (Takashi, 1979) and 0.285 (Miki and Wahl, 1984), respectively. The fundamental anisotropies of IAEDANS and IAF have been reported to be 0.328 (Hudson and Weber, 1973) and 0.4 (Chen and Bowman, 1965), respectively. These values give a maximum error range for the critical distance (R_0) calculated by using κ^2 = ⅔ of ~30%, i.e., the calculated range appears to be unacceptably large. It should be noted, however, that the extreme values of R_0 correspond to extreme cases in which the axes of the cones in which the donor and acceptor transition moments rotate rapidly are oriented entirely in unique directions, i.e., perpendicular or parallel to each other. In this calculation, depolarization due to segmental motions of macromolecules (in the time range of 10^{-8} to 10^{-6} s) are not taken into account in estimating the orientation of the transition moments.

Proteins are flexible rather than rigid macromolecules and, therefore, the directions of the transition moments of the probes are probably randomized because of segmental motions. Moreover, in the acto-S1(D) rigor complex, FRET will occur from the probe on SH1 of one S1(D) to its two neighboring S1(A), except in the presence of excess F-actin, which tends to average the range of possible κ^2-values. The real range of κ^2 is thus probably much narrower, and consequently we can expect a concomitant increase in the accuracy of the measured distances.

We have pointed out elsewhere (Miki et al., 1992) that reasonable agreement was obtained between intramolecular distances determined by FRET assuming κ^2 = ⅔. More recently, good agreement was reported between the radial coordinates of specific labels on F-actin and x-ray diffraction data from aligned F-actin (Holmes et al., 1990; dos Remedios and Moens, 1995a). Thus there is mounting evidence for agreement between FRET data, for which interprobe distances have been calculated assuming κ^2 = ⅔, and the same dimension determined by x-ray diffraction.

Experimental conditions for FRET measurements

In the titration experiments shown in Figs. 3–7, we added a small volume of concentrated F-actin stepwise to a D- and A-labeled S1 (and/or HMM) solution and measured the fluorescence intensity of the donor. Although we intended to measure the interhead distance in the rigor complex, a low concentration of ATP remained in the F-actin solution, which would have allowed repeated detachment and reattachment of heads, so as to randomize binding accompanying the hydrolysis of ATP every time F-actin was added. We believe this procedure was especially important for achieving random, nonclustered binding at molar ratios of F-actin to heads greater than 1.

As a consequence, there is a stepwise accumulation of the products of ATP hydrolysis such that at an actin:S1 molar ratio of 1, the ADP concentration would be $\sim 4 \times 10^{-6}$ M. However, the dissociation constant of ADP for the acto-S1 complex and myofibrils is $\sim 2 \times 10^{-4}$ M (White and Taylor, 1976; Greene and Eisenberg, 1980; Johnson and Adams, 1984). We estimate that only $\sim 2\%$ ($= 100 \times (4 \times 10^{-6})/(2 \times 10^{-4})$) of the rigor complex will have bound ADP. Thus we conclude that the actomyosin complexes in our experiments were exclusively in a rigor state.

Interhead distances between S1 and HMM attached to F-actin

No energy transfer was detected between probes on the two heads of HMM that were not attached to F-actin. Because the R_0 for our probe pair is 4.81 nm, the donor and acceptor probes cannot be closer than ~8 nm in solution. This result is consistent with previous reports that the interhead distance between homologous light chains located at the neck region of (scallop) myosin was too great to be detected by the FRET method (Chantler and Tao, 1986), and that the two heads of myosin in the thick filaments in the relaxed state are mobile (Kinosita et al., 1984; Ishiwata et al., 1987a). Consequently, two heads of myosin are, on average, widely separated in solution.

On the other hand, in the rigor complex, Katayama and Wakabayashi (1981) analyzed the three-dimensional image of the acto-HMM rigor complex and concluded that there is little difference in the conformations of the two heads of HMM and that both bind to the homostrand of the two-start F-actin helix (see also Craig et al., 1980). This is consistent with our data. We found that the calculated distances between two SH1 probes on HMM(D) and HMM(A), S1(D) and HMM(A), and S1(A) and HMM(D) were 6.0, 6.3, and 6.1 nm, respectively, being consistent with the 6.2 nm between S1(D) and S1(A) (Fig. 8). Thus the interhead distances did not appear to depend on whether the myosin head was free (S1) or attached to another head (HMM).

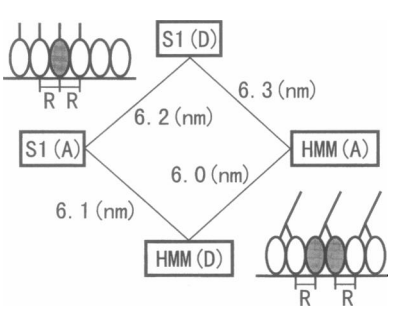

FIGURE 8 The distances between S1 molecules and the heads of HMM molecules attached to F-actin, estimated by model simulation. The binding geometry of S1 and HMM molecules is illustrated schematically in the upper left-hand and lower right-hand portions of the figure. S1 is shown as an oval with a short tail, and HMM is illustrated as two ovals connected by a Y-shaped tail. Filled and unfilled ovals represent D-labeled and A-labeled heads, respectively.

Taken together, these observations indicate that the two heads of HMM must bind to successive monomers along the same long pitch helix of F-actin and that there is no gross distortion in the two heads of HMM, at least around the tip portion containing SH1 groups, when they bind to F-actin. The only exception, as discussed below, is the case in which HMM contains both a donor and an acceptor.

It is noteworthy that, in the case of S1, the calculated curves deviated significantly from the data points when the concentration of actin exceeded that of S1 (Figs. 3–5). These results may be partly attributable to the existence of S1 heads that changed their position/orientation, leading to an increase in the donor-acceptor distance by 1) binding with an altered head orientation (Andreev and Borejdo, 1992; Xiao et al., 1995) and/or 2) bundling formation of actin filaments (Ando and Scales, 1985), both of which occur only at molar ratios of actin/S1 > 1. In contrast, the fit was much better for HMM (Fig. 6), suggesting that the altered head orientation may be characteristic of S1.

The radial coordinate, q (Fig. 2), was estimated from the interhead distances ($R = 6.0–6.3$ nm) to be 5.0–6.4 nm. The accuracy of this estimate is lower than that of R, e.g., a variation of 0.1 nm of R (at around 6.0 nm of R) corresponds to ~0.4 nm of q. It should also be noted that, were the position of SH1 to be distributed around the average position, the FRET distance would represent a lower bound because FRET efficiency depends on the inverse sixth power of R.

Intramolecular interhead distance of HMM attached to F-actin

The unexpected and most interesting consequence of our data is the estimate of the intramolecular interhead distance of HMM molecules attached to F-actin. To estimate this distance, we prepared HMM double-labeled with D and A. The model simulation showed that the average interhead distance was longer than the intermolecular interhead distance, R_{inter}, estimated using HMM(D) and HMM(A). This result was not anticipated because the intramolecular interhead distance, R_{intra}, was expected to be somewhat shorter. In fact, Onishi et al. (Onishi et al., 1989; Onishi and Fujiwara, 1990), using a cross-linking technique, demonstrated that intramolecular head-to-head contact occurs in the complex of smooth muscle HMM and F-actin.

Fig. 9 is a schematic interpretation of HMM results in which shaded and unshaded ovals represent donor-labeled and acceptor-labeled heads, respectively. HMM is shown as two oval heads connected by a Y-piece. In Fig. 9 *a*, the two heads of HMM are separated by a longer distance, R_{intra}, than R_{inter}. In this case, a straightforward interpretation is that the F-actin/HMM complex is distorted so as to make the R_{intra} longer than R_{inter}. This interpretation is realistic because some distortion of the molecule is expected to occur when the second head of an HMM molecule is bound to F-actin. However, in this case, the q and/or ϕ defined in

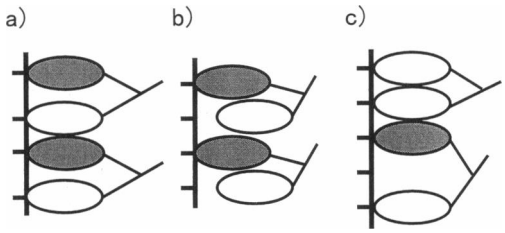

FIGURE 9 An illustration showing three possible interpretations of the model simulations of the binding geometry of HMM(D/A) to F-actin. The intramolecular interhead distance (R_{intra}) is longer than the intermolecular interhead distance (R_{inter}) because of (*a*) the distortion of the structure of an F-actin/HMM complex; (*b*) one-head binding; or (*c*) second-nearest neighbor binding. In the cases of *a* and *c*, R_{intra} is actually longer than R_{inter}. On the other hand, in the case of *b*, the average interhead distance (R_{intra} + R_{inter})/2) is longer than that in the F-actin-HMM (D or A) complex.

Fig. 2 should change, and such changes might be detectable by electron microscopy and/or x-ray fiber diffraction.

A second and more plausible interpretation of our data is illustrated in Fig. 9 *b*. In this scheme, the distances R_{intra} and R_{inter} do not differ, and the binding constant of the acceptor-labeled head for F-actin is effectively decreased because of the heterogeneous labeling. Thus the apparent binding constant of HMM(D/A) molecules will become different from that of HMM(D) or HMM(A). The slight curve observed between molar ratios of 0 and 1 in Figs. 3 and 6 can be more precisely simulated by assuming that the D-labeled heads have a binding constant a few times greater than that of both the A-labeled heads and the unlabeled heads. The tendencies of the data to be convex or concave, as shown in Figs. 4 and 5, are attributable mainly to the higher binding constant of HMM as compared to S1. Thus we speculate that in HMM, in which each head carries a donor or acceptor label (HMM(D/A)), the first head to bind is predominantly D-labeled and the binding equilibrium of the second A-labeled head is reduced, as shown in Fig. 9 *b*. Such single-head binding may be analogous to that previously suggested as the binding mode of HMM with F-actin in the presence of sub-mM PPi (Fujime et al., 1972).

A third interpretation is shown schematically in Fig. 9 *c*. The two heads of HMM(D/A) molecules are assumed to bind to F-actin, along a long strand, to every other actin molecule because of the heterogeneity of the labeled heads. If only 10% of HMM molecules attach to F-actin as shown in Fig. 9 *c*, such that the light scattering determination of the binding stoichiometry is not affected, this would explain the observed increase in the intra-HMM distances (because fluorescence is an average measurement).

CONCLUSIONS

We describe a new method for analyzing FRET data. This method is a potentially powerful tool for analyzing the separate contributions of intramolecular and intermolecular interhead distances from observed fluorescence intensities of S1 and HMM attached to F-actin.

We have demonstrated that under rigor conditions, the interhead distance between SH1 loci is very large in free solution and that the distance (6.0–6.3 nm) between HMM heads attached to F-actin is consistent with their sequential attachment to successive actin monomers along the long-pitch helix of the actin filament. This distance appears to be significantly greater when measured between the two heads of (double-labeled) HMM.

This structural approach was used to analyze the myosin heads interacting with F-actin in the absence of Mg-ATP and is applicable to other states in the kinetic cycle of Mg-ATP hydrolysis.

This paper is dedicated to the memory of Jack Seidel, one of the pioneers in the study of myosin sulfhydryl groups.

A preliminary but essential part of this work was performed in Sydney while one of the authors (SI) was participating in an exchange program for faculty members between the University of Sydney and Waseda University. We thank both universities. We are grateful to Dr. W. Gratzer for his helpful comments on a preliminary version of the manuscript. We also thank the reviewers for their valuable comments.

This work was partially supported by the Ministry of Education, Science, Sports and Culture of Japan, and CREST of Japan, and by a project grant from the National Health and Medical Council of Australia.

REFERENCES

Ando, T., and D. Scales. 1985. Skeletal muscle myosin subfragment-1 induces bundle formation by actin filaments. *J. Biol. Chem.* 260: 2321–2327.

Andreev, O. A., and J. Borejdo. 1992. Two different acto-S1 complexes. *J. Muscle Res. Cell Motil.* 13:523–533.

Brown, L., and B. Hambly. 1996. Distance between the alkali light chains of myosin subfragment-1 bound to F-actin measured using fluorescence spectroscopy. *Biophys. J.* 70:A264. (Abstr.)

Chantler, P. D., and T. Tao. 1986. Interhead fluorescence energy transfer between probes attached to translationally equivalent sites on the regulatory light chains of scallop myosin. *J. Mol. Biol.* 192:87–99.

Chen, R. F., and R. L. Bowman. 1965. Fluorescence polarization measurement with ultraviolet polarizing filters in a spectrophotofluorometer. *Science.* 147:729–732.

Craig, R., A. G. Szent-Györgyi, L. Beese, P. Flicker, P. Vibert, and C. Cohen. 1980. Electron microscopy of thin filaments decorated with a Ca^{2+}-regulated myosin. *J. Mol. Biol.* 140:35–55.

Dale, R. E., J. Eisinger, and W. E. Blumberg. 1979. Orientational freedom of molecular probes. Orientation factor in intramolecular energy transfer. *Biophys. J.* 26:161–194.

dos Remedios, C. G., M. Miki, and J. A. Barden. 1987. Fluorescence resonance energy transfer measurements of distances in actin and myosin. A critical evaluation. *J. Muscle Res. Cell Motil.* 8:97–117.

dos Remedios, C. G., and P. D. J. Moens. 1995a. Actin and the actomyosin interface: a review. *Biochim. Biophys. Acta.* 1228:99–124.

dos Remedios, C. G., and P. D. J. Moens. 1995b. Fluorescence resonance energy transfer spectroscopy is a reliable "ruler" for measuring structural changes in proteins. Dispelling the problem of the unknown orientation factor. *J. Struct. Biol.* 115:175–185.

Förster, T. 1965. Delocalized excitation and excitation transfer. *In* Modern Quantum Chemistry. O. Sinanoglu, editor. Academic Press, New York. 93–137.

Fujime, S., S. Ishiwata, and T. Maeda. 1972. F-actin-heavy meromyosin complex studied by optical homodyne and heterodyne methods. *Biochim. Biophys. Acta.* 283:351–363.

Greene, L. E., and E. Eisenberg. 1980. Dissociation of the actin-subfragment 1 complex by adenyl-5′-yl imidodiphosphate, ADP, and PPi. *J. Biol. Chem.* 255:543–548.

Highsmith, S. 1977. The effects of temperature and salts on myosin subfragment-1 and F-actin association. *Arch. Biochem. Biophys.* 180: 404–408.

Highsmith, S. 1978. Heavy meromyosin binds actin with negative cooperativity. *Biochemistry.* 17:22–26.

Holmes, K. C., D. Popp, W. Gebhard, and W. Kabsch. 1990. Atomic model of the actin filament. *Nature.* 347:44–49.

Hudson, E. N., and G. Weber. 1973. Synthesis and characterization of two fluorescent sulfhydryl reagents. *Biochemistry.* 12:4154–4161.

Ishiwata, S., K. Kinosita, Jr., H. Yoshimura, and A. Ikegami. 1987a. Rotational motions of myosin heads in myofibril studied by phosphorescence anisotropy decay measurements. *J. Biol. Chem.* 262: 8314–8317.

Ishiwata, S., M. Miki, and C. G. dos Remedios. 1987b. Measurement of inter-head distance of myosin using fluorescence energy transfer method. *Biophys. Suppl. (Japanese).* 27:S86. (Abstr.)

Ishiwata, S., M. Miki, T. Funatsu, and C. G. dos Remedios. 1988. Fluorescence energy transfer between heads of myosin bound to F-actin under rigor condition. Proceedings of the 2nd Japan-China Bilateral Symposium on Biophysics, pp. 293–294.

Ishiwata, S., M. Miki, I. Shin, T. Funatsu, K. Yasuda, and C. G. dos Remedios. 1996. Distance between myosin heads in rigor complex measured by fluorescence resonance energy transfer. *Biophys. J.* 70: A14. (Abstr.)

Johnson, R. E., and P. H. Adams. 1984. ADP binds similarly to rigor muscle myofibrils and to actomyosin-subfragment one. *FEBS Lett.* 174: 11–14.

Kabsch, W., H. G. Mannherz, D. Suck, E. F. Pai, and K. C. Holmes. 1990. Atomic structure of the actin:DNase I complex. *Nature.* 347:37–44.

Kasprzak, A. A., R. Takashi, and M. F. Morales. 1988. Orientation of the actin monomer in the F-actin filament: radial coordinate of glutamine-41 and effect of myosin subfragment-1 binding on the monomer orientation. *Biochemistry.* 27:4512–4522.

Katayama, E., and T. Wakabayashi. 1981. Three-dimensional image-analysis of the complex of thin filaments and myosin molecules from skeletal muscle. III. The multi-domain structure of actin heavy meromyosin complex. *J. Biochem.* 90:703–714.

Kielley, W. W., and L. B. Bradley. 1956. The relation between sulfhydryl groups and the activation of myosin adenosinetriphosphatase. *J. Biol. Chem.* 218:653–659.

Kinosita, Jr., K., S. Ishiwata, H. Yoshimura, H. Asai, and A. Ikegami. 1984. Submicrosecond and microsecond rotational motions of myosin head in solution and in myosin synthetic filaments as revealed by time-resolved optical anisotropy decay measurements. *Biochemistry.* 23:5963–5975.

Laemmli, U. K. 1970. Cleavage of structural proteins during the assembly of the head of bacteriophage T4. *Nature.* 227:680–685.

Lehrer, S. S., and G. Kerwar. 1972. Intrinsic fluorescence of actin. *Biochemistry.* 11:1211–1217.

Lorenz, M., D. Popp, and K. C. Holmes. 1993. Refinement of the F-actin model against x-ray fiber diffraction data by the use of a directed mutation algorithm. *J. Mol. Biol.* 234:826–836.

Margossian, S. S., and S. Lowey. 1978. Interaction of myosin subfragments with F-actin. *Biochemistry.* 17:5431–5439.

Marston, S., and A. Weber. 1975. The dissociation constant of the actin-heavy meromyosin subfragment-1 complex. *Biochemistry.* 14: 3868–3873.

McLaughlin, P. J., J. T. Gooch, H.-G. Mannherz, and A. G. Weeds. 1993. Structure of gelsolin segment 1-actin complex and the mechanism of filament severing. *Nature.* 364:685–692.

Miki, M. 1987. The recovery of the polymerization of Lys-61-labeled actin by the addition of phalloidin. *Eur. J. Biochem.* 164:229–235.

Miki, M., S. I. O'Donoghue, and C. G. dos Remedios. 1992. Structure of actin observed by fluorescence resonance energy transfer spectroscopy. *J. Muscle Res. Cell Motil.* 13:132–145.

Miki, M., and P. Wahl. 1984. Fluorescence energy transfer between points in acto-subfragment-1 rigor complex. *Biochim. Biophys. Acta.* 790: 275–283.

Miyanishi, T., and J. Borejdo. 1989. Differential behavior of two cysteine residues on the myosin head in muscle fibers. *Biochemistry.* 28: 1287–1294.

Moens, P. D. J., D. J. Yee, and C. G. dos Remedios. 1994. Determination of the radial coordinate of Cys-374 in F-actin using fluorescence resonance energy transfer spectroscopy: effect of phalloidin on polymer assembly. *Biochemistry.* 33:13102–13108.

Onishi, H., and K. Fujiwara. 1990. The rigor configuration of smooth muscle heavy meromyosin trapped by a zero-length cross-linker. *Biochemistry.* 29:3013–3023.

Onishi, H., T. Maita, G. Matsuda, and K. Fujiwara. 1989. Evidence for the association between two myosin heads in rigor acto-smooth muscle heavy meromyosin. *Biochemistry.* 28:1898–1904.

Rayment, I., H. M. Holden, M. Whittaker, C. B. Yohn, M. Lorenz, K. C. Holmes, and R. A. Milligan. 1993a. Structure of the actin-myosin complex and its implications for muscle contraction. *Science.* 261:58–65.

Rayment, I., W. R. Rypniewski, K. Schmidt-Base, R. Smith, D. R. Tomchick, M. M. Benning, D. A. Winkelmann, G. Wesenberg, and H. M. Holden. 1993b. Three-dimensional structure of myosin subfragment-1: a molecular motor. *Science.* 261:50–58.

Schröder, R. R., D. J. Manstein, W. Jahn, H. Holden, I. Rayment, K. C. Holmes, and J. A. Spudich. 1993. Three-dimensional atomic model of F-actin decorated with *Dictyostelium* myosin S1. *Nature.* 364:171–174.

Schutt, C. E., J. C. Myslik, M. D. Rozycki, N. C. W. Goonesekere, and U. Lindberg. 1993. The structure of crystalline profilin-β-actin. *Nature.* 365:810–816.

Seidel, J. C. 1969. Similar effects on enzymic activity due to chemical modification of either of two sulfhydryl groups of myosin. *Biochim. Biophys. Acta.* 180:216–219.

Sekine, T., and W. W. Kielley. 1964. Enzymic properties of *N*-ethylmaleimide modified myosin. *Biochim. Biophys. Acta.* 81:336–345.

Sutoh, K. 1981. Location of SH1 and SH2 along a heavy chain of myosin subfragment 1. *Biochemistry.* 20:3281–3285.

Sutoh, K., K. Yamamoto, and T. Wakabayashi. 1984. Electron microscopic visualization of the SH1 thiol of myosin by the use of an avidin-biotin system. *J. Mol. Biol.* 178:323–339.

Sutoh, K., K. Yamamoto, and T. Wakabayashi. 1986. Electron microscopic visualization of the ATPase site of myosin by photoaffinity labeling with a biotinylated photoreactive ATP analog. *Proc. Natl. Acad. Sci. USA.* 83:212–216.

Takashi, R. 1979. Fluorescence energy transfer between subfragment-1 and actin points in the rigor complex of acto subfragment-1. *Biochemistry.* 18:5164–5169.

Taylor, D. L., J. Reidler, J. A. Spudich, and L. Stryer. 1981. Detection of actin assembly by fluorescence energy transfer. *J. Cell Biol.* 89: 362–367.

Tirion, M. M., D. ben-Avraham, M. Lorenz, and K. C. Holmes. 1995. Normal modes as refinement parameters for the F-actin model. *Biophys. J.* 68:5–12.

Tokunaga, M., K. Sutoh, C. Toyoshima, and T. Wakabayashi. 1987. Location of the ATPase site of myosin determined by three-dimensional electron microscopy. *Nature.* 329:635–638.

Toyoshima, C., K. Yamamoto, K. Sutoh, T. Sekine, and T. Wakabayashi. 1985. Three-dimensional image analysis of the actin-tropomyosin-myosin subfragment-1 complex: location of specifically reactive thiol SH1. Proceedings of Yamada Conference XI on Energy Transduction in ATPases. Y. Mukohata, M. F. Morales, and S. Fleischer, editors. Yamada Science Foundation, Osaka. 162–163.

Weeds, A. G., and B. Pope. 1977. Studies on the chymotryptic digestion of myosin. Effects of divalent cations on proteolytic susceptibility. *J. Mol. Biol.* 111:129–157.

White, H. D., and E. W. Taylor. 1976. Energetics and mechanism of actomyosin adenosine triphosphatase. *Biochemistry.* 15:5818–5826.

Xiao, M., Andreev, O. A., and J. Borejdo. 1995. Rigor cross-bridges bind to two actin monomers in thin filaments of rabbit psoas muscle. *J. Mol. Biol.* 248:294–307.